Performance Evaluation and Parameter Optimization of MC-CDMA

Mamoun Guenach, *Member, IEEE*, and Heidi Steendam, *Member, IEEE*

***Abstract*—The performance of multicarrier systems depends on the propagation channel behavior. The latter is subject to time and/or frequency selectivity. The designer has to select properly the guard interval and the number of carriers for a given system bandwidth to combat the channel dispersiveness. In this paper, we investigate the sensitivity of downlink multicarrier code-division multiple-access (MC-CDMA) performance to these parameters in different environments. We derive closed-form expressions of the useful and the different interference powers after maximum ratio combining and despreading. The optimum parameters correspond to the minimum of the signal-to-noise-ratio degradation. It turns out that the derivations in the paper of Steendam and Moeneclaey (*IEEE Trans. Commun.*, 1999) that are restricted to the orthogonal frequency-division multiplexing (OFDM) system are a particular case of our results. Numerical evaluation of the analytical expressions reveals that the optimum parameters of the MC-CDMA and its corresponding OFDM system are similar and depend in the same way on the channel characteristics. We show in this paper that the load of the MC-CDMA system only has small influence on the optimization of the parameters. Therefore, from the point of view of parameter optimization, single-user transmission is sufficient to find the optimum parameters. Furthermore, as the optimum parameters mainly depend on the channel characteristics, similar conclusions can be drawn for the uplink transmission.**

***Index Terms*—Fading channels, multicarrier code-division multiple-access (MC-CDMA), orthogonal frequency-division multiplexing (OFDM), performance optimization.**

I. Introduction

MULTICARRIER systems have emerged as a powerful candidate to wireless communication systems. The orthogonal frequency-division multiplexing (OFDM) technique was selected as a transmission standard technique in digital audio broadcasting from satellite or fixed terrestrial to mobile users [2] and in digital video broadcasting in Europe [3]. Another important application of MC systems can be found in transmission of high data rate over twisted pair [4]. So far, the conventional code-division multiple-access (CDMA) technique that is the core wireless technology in the third generation is limited by channel dispersion, causing intersymbol interference (ISI), which requires advanced detection algorithms to be removed. The combination of OFDM and CDMA, i.e., multicarrier (MC) CDMA [5], has drawn a lot of attention due to its robustness to channel dispersion, hence ISI, and its ability to accommodate a higher number of users as compared to CDMA only. Basically, we can distinguish three versions, namely: 1) MC-CDMA, 2) MC direct-sequence CDMA, and 3) multitone CDMA [5].

The robustness of the MC systems to the channel frequency selectivity that induces intercarrier interference (ICI) (which is caused by other carriers from the same MC symbol) and ISI (which is caused by other MC symbols) is obtained by transmitting the data over subchannels with a very low bandwidth as compared to the total system bandwidth. If the subchannel bandwidth is smaller than the channel coherence bandwidth (CB), the interference can be removed completely after the fast Fourier transform (FFT) at the receiver. Otherwise, the interference can be reduced by adding a guard interval per MC symbol. The subchannel bandwidth is proportional to the inverse of the MC symbol period. Therefore, increasing this parameter will reduce the interference level at the input of the decision device. However, there is another constraint that should be fulfilled to avoid interference caused by the time selectivity of the channel: The MC symbol duration has to be smaller than the channel coherence time (CT) duration related to the time variation of the channel. If this condition is not respected, ICI will be introduced.

Hence, the designer has to select the optimum parameters according to a certain criterion. The few contributions found in the literature deal with the OFDM parameter optimization. In [3] and [6], the optimum number of OFDM subchannels is found in the absence of the ISI; i.e., the guard interval is sufficiently high to cope with the ISI. In [7], an OFDM system is investigated in the presence of ICI and ISI. In [1], the authors compute the useful and interference powers due to ICI and ISI. In the previous contributions, a Rayleigh fading channel with 2-D scattering is assumed. In [8], the authors extend the work done in [1] to evaluate the performance of OFDM systems on mobile radio propagation environment considering 3-D scattering.

In this paper, we extend the work done in [1] to downlink MC-CDMA systems equipped with the maximum ratio combining (MRC) equalizer and using Walsh–Hadamard codes with a random overlay sequence as spreading codes. The results obtained in [1] for the OFDM system can be seen as a particular case of our MC-CDMA system with a processing gain of one and will serve as a reference system. The main goal of this paper is to provide the designer with practical rules and analytical tools rather than to resort to simulations to find the optimum

Manuscript received April 28, 2005; revised November 16, 2005, June 8, 2006, and July 16, 2006. The review of this paper was coordinated by Prof. J. H. Cho.

The authors are with the Department of Telecommunications and Information Processing, Ghent University, 9000 Gent, Belgium (e-mail: guenach@telin.UGent.be; hs@telin.UGent.be).

Color version of one or more of the figures in this paper are available online at http://ieeexplore.ieee.org.

Digital Object Identifier 10.1109/TVT.2007.895605

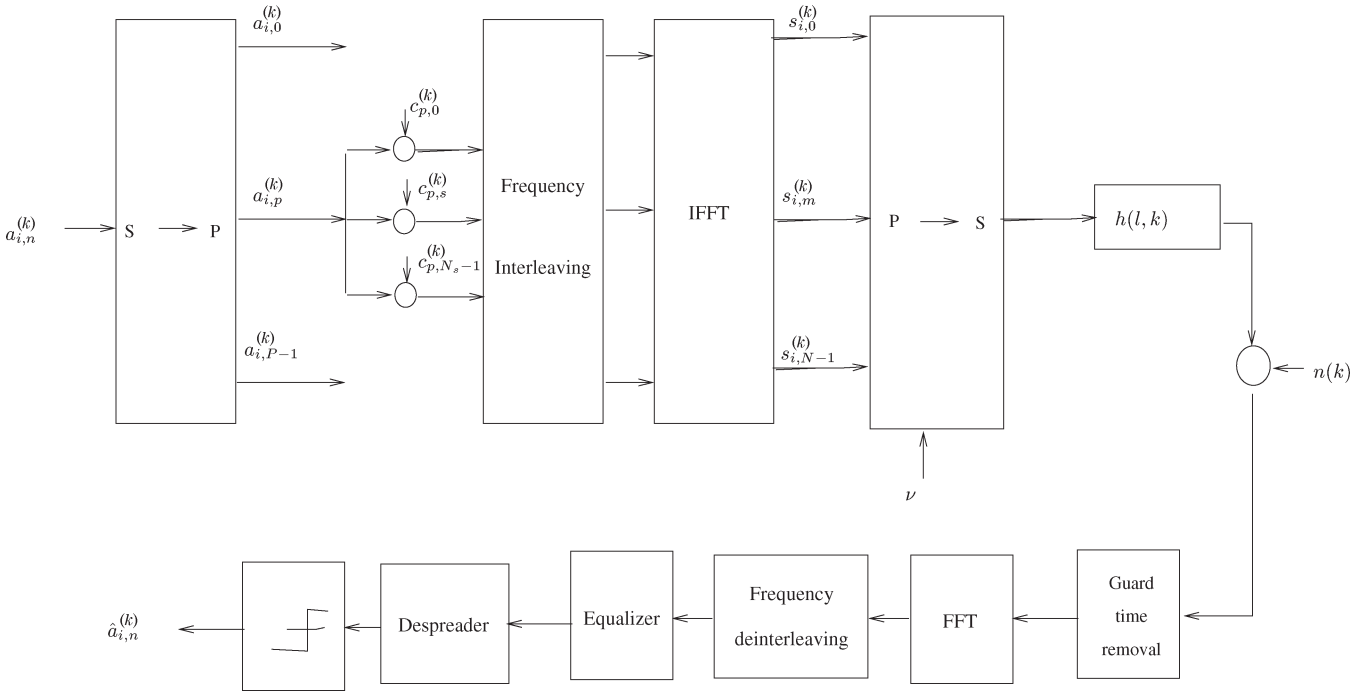

Fig. 1. Transceiver-end flowchart.

set of parameters for a given system. For this purpose, we derive analytical expressions for the useful and interference powers and the signal-to-noise-ratio degradation (SNRD) after MRC equalization and despreading. The SNRD will serve as a cost function to be minimized to find the optimum number of carriers and guard interval. In the numerical evaluation, we consider different propagation environments to come up with general optimization rules that are channel independent. In this paper, we show that the optimum parameters for downlink transmission only depend on the channel characteristics and not on the load of the MC-CDMA system. Therefore, from the point of view of parameter optimization, single-user transmission can be considered. For the uplink transmission, similar conclusions can be drawn. As the optimum parameters depend only on the channel and not on the load of the MC-CDMA system, the optimum parameters for the uplink transmission are (essentially) the same as for the downlink transmission. Furthermore, as in the downlink transmission, single-user transmission will be sufficient to determine the optimum parameters.

The outline of this paper is as follows: First, the system model is described in Section II. In Section III, we derive analytical expressions for the useful power, the interference power, and the SNRD. Numerical evaluations can be found in Section IV, before we conclude in Section V.

II. System Model

The block diagram of the MC-CDMA downlink transceiver with K_u active users is sketched in Fig. 1. After serial-to-parallel conversion of P symbols, the pth symbol of the kth user in the ith block $a_{i,p}^{(k)}$ is spread by the user-specific spreading sequence $c_{p,s}^{(k)}$ that repeats from frame to frame, with $p = 0, \ldots, P-1$ and $s = 0, \ldots, N_s - 1$, where N_s is the spreading factor. Each chip $a_{i,p}^{(k)} c_{p,s}^{(k)}$ is mapped to a carrier denoted $n_{p,s}^{(k)}$, where $0 \le n_{p,s}^{(k)} \le N-1$. In total, we have $N = PN_s$ carriers. To achieve frequency diversity, the assignment of the carriers to chips is made such that the frequency separation among carriers conveying the chips of the same data symbol is maximized. One possible mapping is as follows: The pth data stream is transmitted on N_s carriers with frequencies $f_{p+sP} = f_c + (p+sP)/(NT)$, i.e., $n_{p,s}^{(k)} = p + sP$, where $1/T$ is the system bandwidth and f_c is the radio-frequency carrier of the MC system. After feeding the ith block of spread data symbols to an inverse FFT of length N, the resulting block of N time-domain samples is cyclically extended by a prefix of ν samples. The mth sample of the resulting MC block of $N+\nu$ samples is given by

$$s_{i,m}^{(k)} = \sqrt{\frac{E_s}{N+\nu}} \sum_{p=0}^{P-1} a_{i,p}^{(k)} \sum_{s=0}^{N_s-1} c_{p,s} \exp\left[j2\pi m \frac{n_{p,s}^{(k)}}{N} \right] \quad m = -\nu, \ldots, N-1. \quad (1)$$

By denoting $h(l;k) = h(\tau = lT; t = kT)$ as the lth channel tap at time instant $t = kT$ of a tapped delay line channel with symbol spacing, the received samples $r(k)$ of the jth frame (after removal of the cyclic prefix) are

$$r(k) = \sum_{u=0}^{K_u-1} \sum_{i=\infty}^{+\infty} \sum_{m=-\nu}^{N-1} s_{i,m}^{(u)} h\left(k - m - i(N+\nu); k\right) + n(k) \quad k = j(N+\nu), \ldots, j(N+\nu) + N - 1. \quad (2)$$

Without loss of generality, we will assume that all users have the same mapping between the chips and the carriers, i.e., $n_{p,s}^{(k)} = n_{p,s}\ \forall k$, and we will concentrate on the MC symbol detection of the first user, i.e., $u = 0$, during the frame $j = 0$. The output $b_{0,p',s'}^{(0)}$ of the FFT corresponding to the chip $a_{0,p'}^{(0)} c_{p',s'}^{(0)}$ can be written as

$$b_{0,p',s'}^{(0)} = \sqrt{\frac{1}{N}} \sum_{k=0}^{N-1} r(k) \exp\Big[-j2\pi k \frac{n_{p',s'}}{N}\Big].$$

After the expansion of the received samples, it can be shown that

$$b_{0,p',s'}^{(0)} = \sqrt{\frac{N}{N+\nu}} E_s \sum_{u=0}^{K_u-1} \sum_{i=-\infty}^{+\infty} \sum_{p=0}^{P-1} \sum_{s=0}^{N_s-1} \times a_{i,p}^{(u)} c_{p,s}^{(u)} \gamma(n_{p',s'}; n_{p,s}; i) + \frac{1}{\sqrt{N}} \sum_{k=0}^{N-1} n(k) \times \exp\Big[-j2\pi k \frac{n_{p',s'}}{N}\Big] \quad (3)$$

where

$$\gamma(n_{p',s'}; n_{p,s}; i) = \frac{1}{N} \sum_{m=-\nu}^{N-1} \sum_{k=0}^{N-1} \exp\Big[-j2\pi \frac{n_{p',s'}k - n_{p,s}m}{N}\Big] \times h(k - m - i(N+\nu); k). \quad (4)$$

Note that the useful part in the FFT output $b_{0,p',s'}^{(u)}$ in (3) can be expressed as

$$\left(b_{0,p',s'}^{(0)}\right)_U = \sqrt{\frac{N}{N+\nu}} E_s a_{0,p'}^{(0)} c_{p',s'}^{(0)} \gamma\left(n_{p',s'}; n_{p',s'}; 0\right). \quad (5)$$

Therefore, the MRC equalizer multiplies the $n_{p',s'}$th FFT output with $d_{0,p',s'} = \gamma^*(n_{p',s'}; n_{p',s'}; 0)$. After MRC and despreading of the different chips related to the symbol index p', the decision variable $y_{0,p'}^{(0)}$ is as follows:

$$y_{0,p'}^{(0)} = \sum_{s'=0}^{N_s-1} \left(c_{p',s'}^{(0)}\right)^* d_{0,p',s'} b_{0,p',s'}^{(0)}. \quad (6)$$

III. Performance Analysis

Based on the decision variable in (6), we can identify three sources of interference on top of the useful component and the additive white Gaussian noise (AWGN) component: 1) the self-ISI (S-ISI) due to the frequency selectivity of the channel, 2) the self-ICI (S-ICI) due to both the time and frequency selectivities of the channel, and 3) the multiple access interference (MAI) due to both the frequency and time selectivities of the channel. The power at the output of the equalizer can be decomposed as $E_s(N/(N+\nu))(P_U + P_{\rm ICI} + P_{\rm ISI} + P_{\rm MAI}) + P_{\rm AWGN}$ where P_X, $X = U, {\rm ICI}, {\rm ISI}, {\rm MAI}, {\rm AWGN}$, corresponds to the useful, S-ICI, S-ISI, MAI, and AWGN powers, respectively, i.e.,

$$P_U = E\left\{\left|\Gamma^{(0,0)}(n_{p'}; n_{p'}; 0)\right|^2\right\} \quad (7)$$

$$P_{\rm ICI} = \sum_{\substack{p=0 \\ p\neq p'}}^{P-1} E\left\{\left|\Gamma^{(0,0)}(n_{p'}; n_p; 0)\right|^2\right\} \quad (8)$$

$$P_{\rm ISI} = \sum_{\substack{i=-\infty \\ i\neq 0}}^{+\infty} \sum_{p=0}^{P-1} E\left\{\left|\Gamma^{(0,0)}(n_{p'}; n_p; i)\right|^2\right\} \quad (9)$$

$$P_{\rm MAI} = \sum_{u=1}^{K_u-1} \sum_{i=-\infty}^{+\infty} \sum_{p=0}^{P-1} E\left\{\left|\Gamma^{(0,u)}(n_{p'}; n_p; i)\right|^2\right\} \quad (10)$$

$$P_{\rm AWGN} = E\Bigg\{\Bigg|\sqrt{\frac{1}{N}} \sum_{s'=0}^{N_s-1} \left(c_{p',s'}^{(0)}\right)^* d_{0,p',s'} \times \sum_{k=0}^{N-1} n(k) \exp[-j2\pi n_{p',s'} k/N]\Bigg|^2\Bigg\} \quad (11)$$

where

$$\Gamma^{(0,u)}(n_{p'}; n_p; i) = \sum_{s',s=0}^{N_s-1} \left(c_{p',s'}^{0}\right)^* c_{p,s}^{(u)} d_{0,p',s'} \gamma(n_{p',s'}; n_{p,s}; i).$$

The averaging in P_X is with respect to the statistics of the data symbols that are supposed to be independent identically distributed with zero mean and unit variance, the fourth-order moments of the spreading chips, and the channel autocorrelation function that depends on the power delay profile and the Doppler spectrum distributions. In the following, we derive closed-form analytical expressions for the useful and interference powers in terms of the wide-sense stationary uncorrelated scatterer channel autocorrelation $R(l;k)$ function that is defined as $E\{h(\tau = lT, t = kT)h^*(\tau' = l'T, t' = k'T)\} = \delta(l-l')R(l;k-k')$. The parameter P_T, which is the total power that is defined as $P_T = P_U + P_{\rm ICI} + P_{\rm ISI} + P_{\rm MAI}$, can be expressed as

$$P_T = \sum_{u=0}^{K_u-1} \sum_{i=-\infty}^{+\infty} \sum_{p=0}^{P-1} E\left\{\left|\Gamma^{(0,u)}(n_{p'}; n_p; i)\right|^2\right\}. \quad (12)$$

Considering Walsh–Hadamard codes with a random overlay sequence, it can be shown that the fourth-order moment statistics of the chips [9] are given by

$$\begin{aligned} E\left\{\left(c_{p',s'}^{(u')}\right)^* c_{p,s}^{(u)} c_{p',s'_1}^{(u')} \left(c_{p,s_1}^{(u)}\right)^*\right\} &\simeq \frac{1}{N_s^2}\delta_{s',s'_1}\delta_{s,s_1} + \frac{1}{N_s^2}\delta_{p',p} \times (\delta_{s',s}\delta_{s_1\prime,s_1} - \delta_{s',s,s'_1,s_1}), \quad \text{if } u' = u \\ &\simeq \frac{1}{N_s^2}\delta_{s',s'_1}\delta_{s,s_1} - \frac{1}{N_s^2}\frac{1}{N_s-1}\delta_{p',p} \times (\delta_{s',s}\delta_{s_1\prime,s_1} - \delta_{s',s,s'_1,s_1}), \quad \text{if } u' \neq u. \end{aligned} \quad (13)$$

Defining

$$X_{p',i} = \sum_{s,s'=0}^{N_s-1} E\left\{|d_{0,p',s'}|^2\,|\gamma(n_{p',s'};n_{p,s};i)|^2\right\}$$

$$Y_{p',p,i} = \sum_{s,s'=0}^{N_s-1} E\{d_{0,p',s'}\gamma(n_{p',s'};n_{p',s'};i) \times d^*_{0,p',s}\gamma^*(n_{p',s};n_{p',s};i)\}$$

$$Z_{p',p,i} = \sum_{s'=0}^{N_s-1} E\left\{|d_{0,p',s'}|^2\,|\gamma(n_{p',s'};n_{p',s'};i)|^2\right\}$$

we can write

$$E\left\{\left|\Gamma^{(u,u)}(n_{p'};n_p;i)\right|^2\right\} = \frac{1}{N_s^2}(X_{p',i}+\delta_{p',p}Y_{p',p,i}-\delta_{p',p}Z_{p',p,i})$$

$$E\left\{\left|\Gamma^{(u,u')}(n_{p'};n_p;i)\right|^2\right\} = \frac{1}{N_s^2}\left(X_{p',i}-\frac{\delta_{p',p}}{N_s-1}Y_{p',p,i}+\frac{\delta_{p',p}}{N_s-1}Z_{p',p,i}\right), \quad \text{if } u' \neq u \tag{14}$$

where the averaging still has to be done over the channel characteristics. We will assume that the channel taps are zero-mean random complex Gaussian variables. Noting that $d_{0,p',s'} = \gamma^*(n_{p',s'};n_{p',s'};0)$ and taking into account (4) and (14), it follows that the computation of P_T and P_U requires the statistical fourth-order moments of the channel taps. To compute these fourth-order moments, we rewrite $\gamma(n_{p',s'};n_{p,s};i)$ as

$$\gamma(n_{p',s'};n_{p,s};i) = \frac{1}{N}\left(\sum_{q=0}^{\nu}\sum_{k=0}^{N-1} + \sum_{q=\nu+1}^{N+\nu-1}\sum_{k=q-\nu}^{N-1} + \sum_{q=-N+1}^{-1}\sum_{k=0}^{N+q-1}\right) \times \exp\left[j2\pi\frac{n_{p,s}(k-q)-n_{p',s'}k}{N}\right] h\left(q-i(N+\nu);k\right). \tag{15}$$

The derivations related to the total and useful powers can be found in the Appendix.

One important parameter in the system performance is the signal-to-noise ratio (SNR), which is the ratio of the useful power and the other sources of interference power, i.e.,

$$\text{SNR} = \frac{E_s\frac{N}{N+\nu}P_U}{E_s\frac{N}{N+\nu}(P_{\text{ICI}}+P_{\text{ISI}}+P_{\text{MAI}})+P_{\text{AWGN}}}. \tag{16}$$

To tackle how the performance degrades in the fading channels as compared to the ideal case, i.e., the equivalent frequency–time flat channels, we define the SNRD as the SNR reduction as compared to the ideal case: $\text{SNRD} = 10\log(\text{SNR}_{\text{AWGN}}/\text{SNR})$. Following the derivations in the Appendix, we end up with (17), which is shown at the bottom of the page, where the multivariate function $w_0(0;q;r)$ can be found in the Appendix. In the following, some special cases are discussed: the OFDM system, the time-flat channel case, and the frequency-flat channel case.

A. OFDM System

The OFDM case corresponds to the case where $N_s = 1$ and $K_u = 1$. The useful and total powers, respectively, reduce to

$$P_U = \frac{2}{N^2}\left\{\sum_{q=-\infty}^{+\infty}\sum_{r=-\infty}^{+\infty} w_0(0;q;r)R(q;r)\right\} \tag{18}$$

and

$$P_T = \frac{1}{N}\sum_{q=-\infty}^{+\infty}\sum_{r=-\infty}^{+\infty} w_0(0;q;r)R(q;r) + \frac{1}{N^2}\sum_{i=-1}^{1}\sum_{p=0}^{P-1}\left|\sum_{q=-\infty}^{+\infty}\sum_{r=-\infty}^{+\infty} w_i(p-p';q;r)R(q;r) \times \exp\left[j2\pi(q+r)\frac{p-p'}{N}\right]\right|^2. \tag{19}$$

Note that the aforementioned expressions differ slightly from the expressions in [1]. This can be explained as follows: In this paper, we computed the useful and interference powers at the output of the equalizer, i.e., after MRC,[1] which corresponds to multiplying each FFT output with the channel coefficient corresponding with the considered carrier. In [1], the useful and total powers are computed before the equalizer at the FFT outputs. However, we have carried out computations for both cases and found very similar optimum parameters for both cases.

[1]Note that in the case of OFDM, the MRC is reduced to a single tap equalizer without any carrier combining.

$$\text{SNRD} = -10\log\left(\frac{\frac{N}{N+\nu}P_U}{2\left(\left[\frac{1}{N}\sum_{q=-\infty}^{+\infty}\sum_{r=-\infty}^{+\infty} w_0(0;q;r)R(q;r)\right] + \frac{E_s}{N_0}\frac{N}{N+\nu}(P_T-P_U)\right)}\right) \tag{17}$$

B. Frequency-Flat Channel and Time-Flat Channel

The expressions of the total power in the *frequency-flat* case [i.e., $R(q,r)=\delta(q)\tilde{R}(r)$] could be simplified because the terms where $w_1(\Delta,q,r)$ and $w_{-1}(\Delta,q,r)$ are present vanish. In the *time-flat* case [i.e., $R(q,r)=\tilde{R}(q)\delta(r)$], only small simplifications are possible. In [1], it is shown for OFDM that the SNRD for a frequency-selective time-selective channel can be obtained by splitting the doubly selective channel into a frequency-flat channel and time-flat channel (with the same time selectivity and frequency selectivity, respectively, as the doubly selective channel). By computing the SNRD for both cases, the SNRD for the doubly selective channel is then obtained by adding the SNRD of the frequency-flat and time-flat counterparts. We have checked by numerical evaluation that this method for computing the SNRD for the doubly selective channel is also valid for the MC-CDMA system from this paper. The relevance of this equivalent representation lays in the fact that the expressions for the powers in the time-flat and frequency-flat cases are less complex than for a doubly selective channel and, hence, less time consuming in the computations. Note that in the time–frequency flat case, we can easily obtain $P_T=P_U=2$, provided that the channel power average is normalized to unity, i.e., $\sum_{q=-\infty}^{+\infty}h(q,0)=1$.

IV. Numerical Results

In this section, we have evaluated the obtained analytical expressions to optimize the system parameters of the MC-CDMA system. The OFDM system will serve as a reference system, and the optimum parameters of the MC-CDMA system will be compared to those of the OFDM system. Two Dopplers are considered, corresponding to mobile speeds of $v=20$ km/h and $v=100$ km/h. The channel impulse response corresponds to a multipath Rayleigh fading channel with a maximum delay spread of $\tau_{\max}=7$ μs and a power delay profile $p_\tau(\tau)=\exp[-\tau/\tau_{\text{slope}}]$, where $\tau_{\text{slope}}=1$ μs. The classical Jakes distribution is assumed for the Doppler frequencies $p_{f_D}(f_D)=1/[\pi f_{D_{\max}}\sqrt{(1-(f_D/f_{D_{\max}})^2)}]$, where $f_{D_{\max}}=(v/c)f_c$ is the maximum Doppler spread and f_c is the carrier frequency. The equivalent autocorrelation function of the channel that is defined as $E\{h(lT,kT)h^*(l'T,k'T)\}=\delta(l-l')R(l;k-k')$ can be written as

$$R(l;k)=\sigma p_\tau(\tau=lT)\int_{-\infty}^{+\infty}p_{f_D}(f)\exp^{j2\pi kfT}\,df$$

where σ is selected such that $\sum_l R(l;0)=1$. Computations are carried out for an MC-CDMA system using Walsh–Hadamard spreading codes of spreading factor $N_s=8$ followed by an overlay random code, a system bandwidth $B=2$ MHz, i.e., $T=0.5$ μs, and a carrier frequency of $f_c=1$ GHz. Based on the selected parameters, we have a tapped delay line channel with $L=15$ taps, that is to say, the index l in $R(l;k)$ ranges between 0 and $L-1$. To compute channel CB and CT, we use the following expressions [10]: $B_c=1/(2\pi\tau_{\max})$ and $T_c=1/(16\pi f_{D_{\max}})$, respectively. It turns out that the CB is $B_c=22.74$ kHz, and the maximum Doppler frequency is $f_{D_{\max}}=92.6$ Hz (resp. 18.52 Hz) for a mobile speed of $v=100$ km/h (resp. $v=20$ km/h), which results in a CT of $T_c=1.9$ ms (resp. $T_c=9.7$ ms). We will refer to the scenario with $v=100$ km/h (resp. $v=20$ km/h) as scenario A (scenario B).

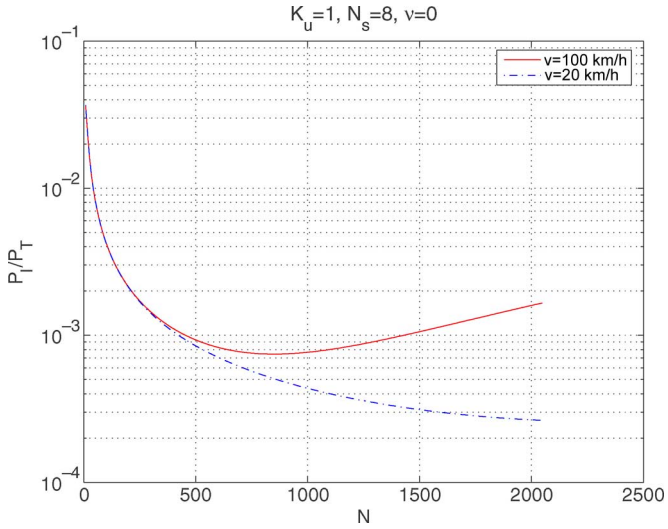

Fig. 2. Normalized interference power in case of mobile speeds of 20 and 100 km/h as a function of the number of carriers for $\nu=0$ and $K_u=1$.

In Fig. 2, the interference power $P_I=P_T-P_U$ is shown as a function of the number of carriers for zero guard interval ($\nu=0$) and single-user transmission $K_u=1$. As can be noticed, the interference power decreases if the number of carriers $N=PN_s$ is below a certain threshold that is defined in general by the CT. A rough approximation of the CT of scenarios A and B gives 1.9 and 9.7 ms, respectively. Taking into account the bandwidth of 2 MHz, the duration of an MC-CDMA block with N carriers and guard interval duration ν is equal to $(N+\nu)T$. Hence, for $\nu=0$, the thresholds for scenarios A and B correspond to a number N of carriers equal to 3800 and 19 000, respectively. As long as the number of carriers is much smaller than this threshold (typically less than 10% of the threshold), increasing N in this region means that the bandwidth per carrier becomes progressively smaller as compared to the channel coherence bandwidth, which helps in combating the interference caused by channel dispersion. Once the N is beyond this critical point, because of the time selectivity of the channel, the channel impulse response is not anymore constant per MC symbol, causing ICI and an increasing amount of interference power P_I. Therefore, for a given guard interval, the interference power reaches its minimum at intermediate values of N, which suggests the existence of optimum parameters that minimize the SNRD.

In Fig. 3, the performance in terms of the interference power as a function of the guard interval ν is shown for $N=256$ and $K_u=1$. As expected, as the guard interval increases, the interference power reduces. The lowest values of P_I are obtained when the guard interval is larger than the maximum delay spread $\tau_{\max}$: $\nu=(\tau_{\max}/T)=14$. Beyond this threshold, the interference power can be considered as negligible, and therefore, for single-user transmission, $P_T=P_U$, which corresponds to the time–frequency flat channel case. However,

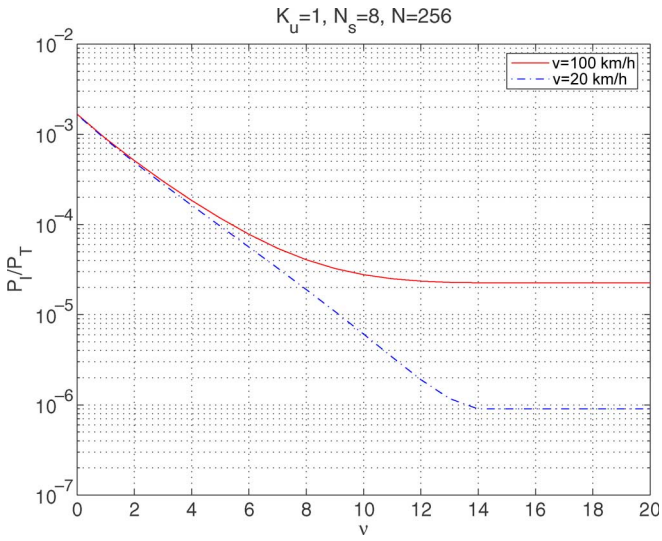

Fig. 3. Normalized interference power in case of mobile speeds of 20 and 100 km/h as a function of the guard interval for $N = 256$ and $K_u = 1$.

the guard interval reduces the throughput and could not be increased without any constraint: The transmitted energy per symbol is proportional to the ratio $N/(N + \nu)$ that decreases when the guard interval increases.

The determinant factor in the system performance is the bit error rate that should be minimized, or equivalently, we have to minimize the SNRD that is defined in (17). In Fig. 4, we plot the optimum number of carriers N (left) and guard interval ν (right) for the MC-CDMA system with $N_s = 8$ and $K_u = 1$, and for the corresponding OFDM system with $N_s = 1$. It can be noticed that the minimization of the SNRD appears to result in different parameters N and ν for the MC-CDMA system and its equivalent OFDM system per E_b/N_0. In the figure, it follows that for all E_s/N_0 operating points, the optimum carrier spacing $(1/NT)_{\text{opt}}$ ranges in the interval $[1/600T, 1/200T]$ for a mobile speed of $v = 100$ km/h and $[1/2000T, 1/400T]$ for a mobile speed of $v = 20$ km/h. It can easily be verified that these optimum carrier spacings are located within the interval determined by the maximum Doppler spread $f_{D_{\max}}$ as a lower bound and the coherence bandwidth, which is inversely proportional to the maximum delay spread $\tau_{\max}$ as an upper bound: $f_{D_{\max}} \ll (1/NT)_{\text{opt}} \ll B_c$.

This can be explained as follows: When the carrier spacing is larger than the Doppler spread, the MC symbol period NT will be smaller than the CT of the channel, such that the channel appears almost time flat to the MC system, reducing the amount of time-selectivity-induced ICI. On the other hand, if the subchannel bandwidth $1/NT$ is smaller than the coherence bandwidth of the channel, the channel is frequency flat per carrier, which is a key factor in MC systems to reduce frequency-selectivity-induced ICI and ISI. It can be noticed that scenario B can accommodate more carriers. This can be explained by the fact that the Doppler spread is smaller as compared to scenario A. On the other hand, for all situations, the optimum guard interval ν_{opt} is not necessarily equal to the maximum delay spread. To completely eliminate the ISI, the guard interval should be at least equal to the channel delay spread, but this will be translated in a system throughput loss. Generally, the optimum ν is a few samples below the maximum delay spread for both scenarios.

In Fig. 4, it follows that the optimum parameters for MC-CDMA and OFDM are similar but not equal. To evaluate the sensitivity of the SNRD to the system parameters, we computed the SNRD for MC-CDMA as a function of the system parameters for scenarios A and B, respectively, single-user transmission, and $E_s/N_0 = 30$ dB. We have carried out the numerical evaluation of the MC-CDMA system by using the optimum parameters for OFDM. We found that the increase in SNRD of the MC-CDMA system (defined as $\text{SNRD} - \text{SNRD}_{\text{opt}}$), which is caused by using the optimum parameters for OFDM instead of the optimum parameters for MC-CDMA, is less than 0.11 and 0.06 dB for scenarios A and B, respectively. From this, we can conclude that the selection of the optimum system parameters is not very critical and that the optimum parameters for OFDM (which are less complex to obtain than for MC-CDMA) can be used in MC-CDMA with only a marginal performance decrease.

This fact is emphasized more explicitly in Fig. 5, where we plot the SNRD as a function of E_s/N_0 for the MC-CDMA system with $N_s = 8$ and $K_u = 1$ for the case where the optimum parameters obtained for MC-CDMA are used and for the case where the optimum parameters for OFDM are used. Hence, for all E_s/N_0, it can be seen that the optimum parameters of the OFDM system and the MC-CDMA system yield almost the same SNRD of the MC-CDMA system. This fundamental result again confirms the rule of thumb when selecting the optimum N and ν.

Fig. 6 illustrates the sensitivity of the optimization to the system load K_u. The number of active users ranges between 1 and N_s, which corresponds to single-user transmission and multiuser transmission, respectively. As can be noticed, for fully loaded system, i.e., $K_u = N_s$, we obtain the optimum parameters that are almost the same as the ones obtained for OFDM optimization, as shown in Fig. 4. This can be explained by the presence of the factor $(N_s - K_u)/(N_s - 1)$ in the expression of the total power (or, equivalently, the interference power) in (29): OFDM (or fully loaded MC-CDMA) system corresponds to the set of parameters $(K_u = N_s = 1)$ [or $(K_u = N_s)$]. All the terms where $(N_s - K_u)/(N_s - 1)$ is present will disappear in these two cases. Besides, all optimum parameters corresponding to a load $1 < K_u < N_s$ (dotted curves with circles and stars in the figure) are located between the bounds corresponding to MC-CDMA single-user transmission and OFDM transmission.

We plot in Fig. 7 the increase in the SNRD with respect to the SNRD_{opt} for a system with a given load when using the optimum parameters obtained for single-user case. As expected, this increase that is defined as $\text{SNRD} - \text{SNRD}_{\text{opt}}$ is small (smaller than 0.003 dB); this confirms that single-user transmission is sufficient when parameter optimization is concerned and that the load has a very limited impact.

V. Conclusion

In this paper, we derived closed analytical expressions for the useful and interference powers of MC-CDMA that can be used

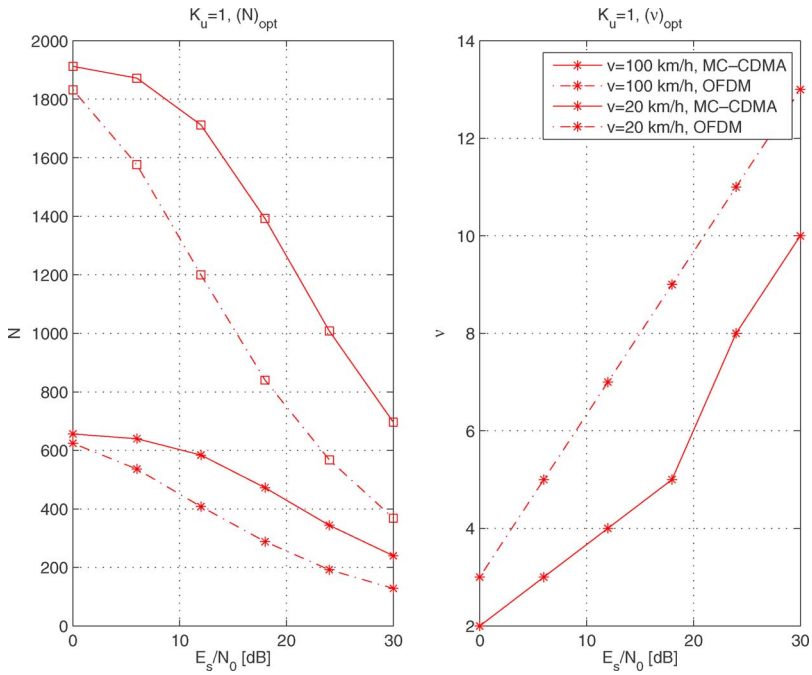

Fig. 4. Optimum number of (left) carriers and (right) guard of interval as a function of E_b/N_0 in case of $K_u = 1$ and mobile speeds of 20 and 100 km/h.

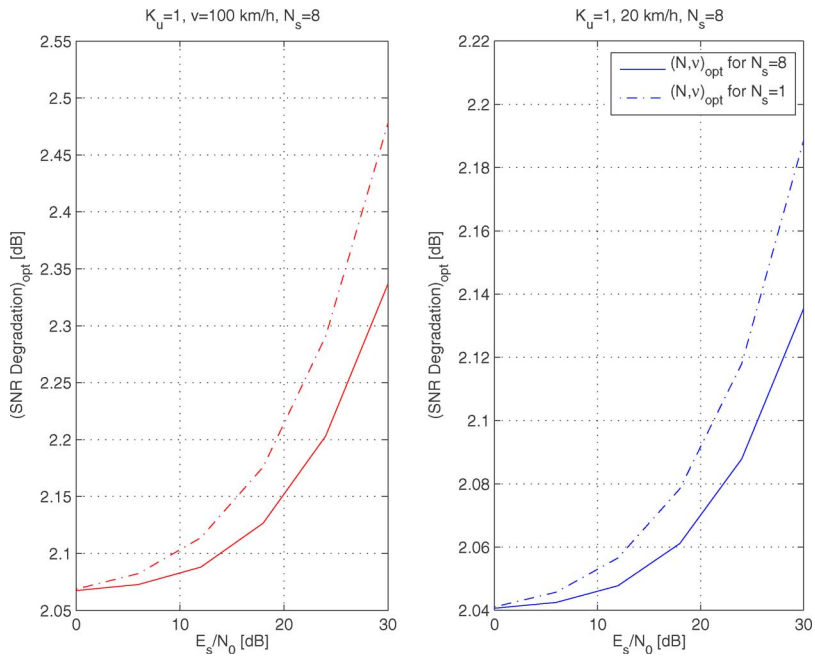

Fig. 5. SNRD of the MC-CDMA system with $N_s = 8$ and $K_u = 1$ in case of mobile speeds of (left) 100 km/h and (right) 20 km/h using the optimum parameters obtained in Fig. 4 and the corresponding ones for the OFDM system.

by the system designer to select the optimum set of parameters. Based on these derivations, we carried out computations to minimize the SNRD and to compute the optimum guard interval and number of carriers. The optimization results of the MC-CDMA were compared to the corresponding OFDM system. Numerical results in different environments confirm the following rule of thumb in selecting the optimum parameters: The carrier spacing should be higher (resp. smaller) as compared to the maximum Doppler (resp. channel coherence bandwidth), whereas the guard interval has to be few samples smaller than the channel delay spread. Comparing the results of the parameter optimization for OFDM and single-user MC-CDMA, and evaluating the sensitivity of the performance on the choice of the system parameters, it turns out that the results obtained for both multicarrier systems are very similar. Moreover, simulation results revealed that the optimum parameters of a fully loaded MC-CDMA system are almost the same as those obtained in its equivalent OFDM system.

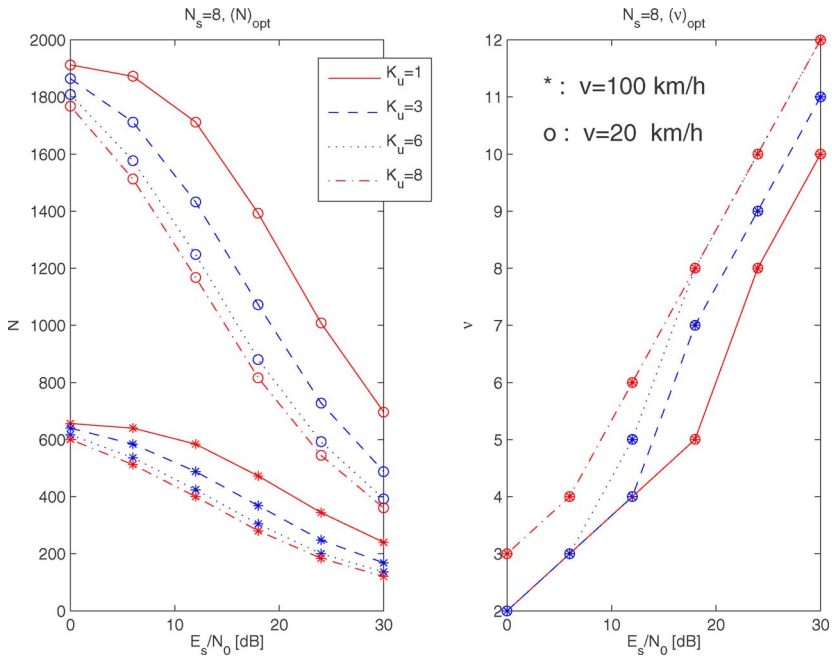

Fig. 6. Optimum number of (left) carriers and (right) guard of interval as a function of E_b/N_0 in case of mobile speeds of 20 and 100 km/h and for both single-user transmission ($K_u = 1$) and multiuser ($K_u > 1$) transmission, respectively.

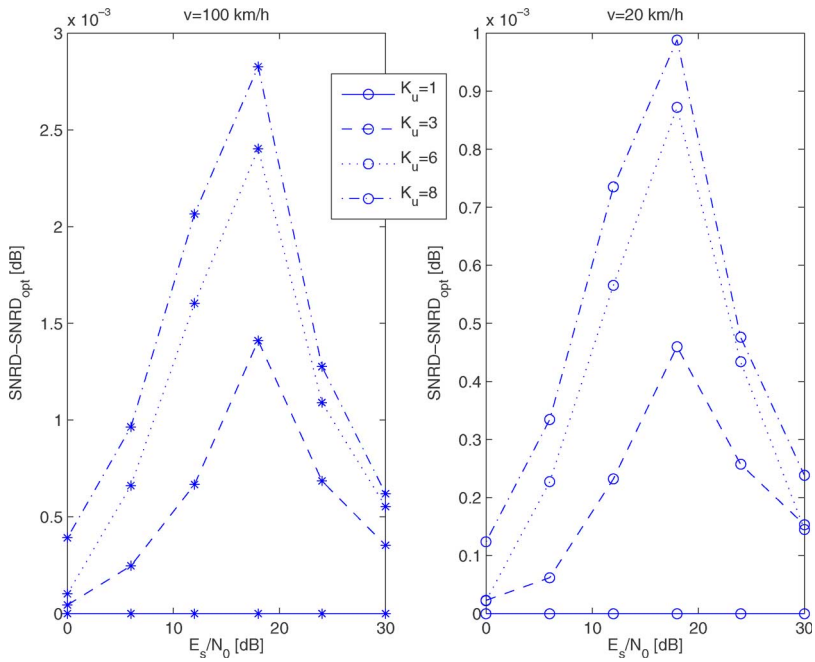

Fig. 7. SNRD increase when using the optimum parameters from single-user transmission to compute the SNRD of MC-CDMA system with a given load K_u.

APPENDIX

Let us define the following useful parameters:

$$S_{k_1,k_2}(\Delta) = \frac{1}{N}\sum_{k=k_1}^{k_2-1}\exp\left[-j2\pi k\frac{\Delta}{N}\right]$$

$$u(r) = \begin{cases} 1, & r \geq 0 \\ 0, & r < 0 \end{cases}.$$

It can be shown that

$$E\left\{\left|\gamma(n_{p',s'};n_{p,s};i)\right|^2\right\} = \frac{1}{N}\sum_{q=-\infty}^{+\infty}\sum_{r=-\infty}^{+\infty} w_0(0;q;r)R\left(q-i(N+\nu);r\right) \times \exp\left[j2\pi r\frac{n_{p,s}-n_{p',s'}}{N}\right] \quad (20)$$

$$E\{\gamma(n_{p',s'};n_{p',s'};i)\gamma^*(n_{p,s};n_{p,s};i)\}$$
$$= \frac{1}{N}\sum_{q=-\infty}^{+\infty}\sum_{r=-\infty}^{+\infty} w_0(0;q;r)R(q-i(N+\nu);r) \times \exp\left[j2\pi q\frac{n_{p,s}-n_{p',s'}}{N}\right] \quad (21)$$

$$E\{\gamma(n_{p',s'};n_{p',s'};0)\gamma^*(n_{p',s'};n_{p,s};i)\}$$
$$= \frac{1}{N}\sum_{q=-\infty}^{+\infty}\sum_{r=-\infty}^{+\infty} w_i(n_{p,s}-n_{p',s'};q;r)\exp\left[j2\pi i n_{p,s}\frac{\nu}{N}\right] \times R(q;r)\exp\left[j2\pi(q+r)\frac{n_{p,s}-n_{p',s'}}{N}\right] \quad (22)$$

where the weight functions $w_i(\Delta;q;r)$ are given in (23)–(25), which are shown at the bottom of the page. Based on the fourth-order statistics of zero-mean Gaussian variables,[2] it can be shown, after some lengthy manipulations, that

$$E\left\{|\gamma(n_{p',s'};n_{p',s'};0)|^2\,|\gamma(n_{p',s'};n_{p,s};i)|^2\right\}$$
$$= \frac{1}{N^2}\left\{\sum_{q=-\infty}^{+\infty}\sum_{r=-\infty}^{+\infty} w_0(0;q;r)R(q-i(N+\nu);r) \times \exp\left[j2\pi r\frac{n_{p,s}-n_{p',s'}}{N}\right]\right\} \times\left\{\sum_{q=-\infty}^{+\infty}\sum_{r=-\infty}^{+\infty} w_0(0;q;r)R(q;r)\right\}$$
$$+\frac{1}{N^2}\left|\sum_{q=-\infty}^{+\infty}\sum_{r=-\infty}^{+\infty} w_i(n_{p,s}-n_{p',s'};q;r) \times\exp\left[j2\pi i n_{p,s}\frac{\nu}{N}\right]R(q;r) \times\exp\left[j2\pi(q+r)\frac{(n_{p,s}-n_{p',s'})}{N}\right]\right|^2 \quad (26)$$

and

$$E\{\gamma^*(n_{p',s'};n_{p',s'};0)\gamma(n_{p',s'};n_{p',s'};i) \times\gamma(n_{p',s};n_{p',s};0)\gamma^*(n_{p',s};n_{p',s};i)\}$$
$$= \frac{1}{N^2}\left\{\sum_{q=-\infty}^{+\infty}\sum_{r=-\infty}^{+\infty} w_0(0;q;r)R(q-i(N+\nu);r) \times\exp\left[j2\pi q\frac{n_{p',s}-n_{p',s'}}{N}\right]\right\} \times\left\{\sum_{q=-\infty}^{+\infty}\sum_{r=-\infty}^{+\infty} w_0(0;q;r)R^*(q;r) \times\exp\left[-j2\pi q\frac{n_{p',s}-n_{p',s'}}{N}\right]\right\}$$
$$+\frac{1}{N^2}\left\{\sum_{q=-\infty}^{+\infty}\sum_{r=-\infty}^{+\infty} w_i(0;q;r)\exp\left[j2\pi i n_{p',s}\frac{\nu}{N}\right]R(q;r)\right\} \times\left\{\sum_{q=-\infty}^{+\infty}\sum_{r=-\infty}^{+\infty} w_i(0;q;r)\exp\left[-j2\pi i n_{p',s'}\frac{\nu}{N}\right]R^*(q;r)\right\} \quad (27)$$

[2]Assume $\alpha_1,\alpha_2,\alpha_3$, and α_4 are complex random variables of which the real and imaginary parts are zero-mean and Gaussian distributed. Then, the fourth order moment $E[\alpha_1\alpha_2\alpha_3\alpha_4]$ can be readily written as $E[\alpha_1\alpha_2\alpha_3\alpha_4] = E[\alpha_1\alpha_2]E[\alpha_3\alpha_4] + E[\alpha_1\alpha_3]E[\alpha_2\alpha_4] + E[\alpha_1\alpha_4]E[\alpha_2\alpha_3]$ [11].

respectively. Starting from the useful and total power expressions in (7) and (12), respectively, and using the fourth-order moment statistics in (26) and (27), we end up with the expressions of the useful and total powers in (28) and (29),

$$w_0(\Delta;q;r) = \exp\left[-j2\pi r\frac{\Delta}{N}u(r)\right]\begin{cases} S_{0,N+q-|r|}, & (1-N\le q\le -1);\quad (|r|\le N-1+q)\\ S_{0,N-|r|}, & (0\le q\le \nu);\quad (|r|\le N-1)\\ S_{q-\nu,N-|r|}, & (\nu+1\le q\le N-1+\nu);\quad (|r|\le N-1+\nu-q)\\ 0, & \text{Otherwise}\end{cases} \quad (23)$$

$$w_1(\Delta;q;r) = \begin{cases} S_{0,N+r}, & (1-N\le q\le -1);\quad (1-N\le r\le \min(q,-N-q))\\ S_{0,N+q}, & (1-N\le q\le -N/2-1);\quad (q+1\le r\le -N-q)\\ -S_{q,q+r}, & (1-N\le q\le -1);\quad (\max(q,-N-q)<r\le -1)\\ -S_{r,q+r}, & (-N/2\le q\le -1);\quad (-N-q+1\le r\le q)\\ 0, & \text{Otherwise}\end{cases} \quad (24)$$

$$w_{-1}(\Delta;q;r) = \begin{cases} S_{q-\nu,q-\nu+r}, & (\nu+1\le q\le N+\nu-1);\quad (1\le r\le \min(q-\nu,N+\nu-q))\\ S_{r,r+q-\nu}, & (\nu+1\le q\le N/2+\nu-1);\quad (q-\nu+1\le r\le N+\nu-q)\\ -S_{N,r}, & (\nu+1\le q\le N+\nu-1);\quad (\max(q-\nu,N+\nu-q)<r\le N-1)\\ -S_{N,q-\nu}, & (N/2+\nu\le q\le N+\nu-1);\quad (N+\nu-q+1\le r\le q-\nu)\\ 0, & \text{Otherwise}\end{cases} \quad (25)$$

$$P_U = \frac{1}{N^2}\left\{\sum_{q=-\infty}^{+\infty}\sum_{r=-\infty}^{+\infty} w_0(0;q;r)R(q;r)\left(\left|\frac{1}{N_s}\sum_{s'=0}^{N_s-1}\exp\left[j2\pi r\frac{n_{p',s'}}{N}\right]\right|^2-\frac{1}{N_s}\right)\right\}\left\{\sum_{q=-\infty}^{+\infty}\sum_{r=-\infty}^{+\infty} w_0(0;q;r)R(q;r)\right\}$$
$$+\frac{1}{N^2N_s^2}\sum_{s',s=0}^{N_s-1}\left|\sum_{q=-\infty}^{+\infty}\sum_{r=-\infty}^{+\infty} w_0(n_{p',s}-n_{p',s'};q;r)R(q;r)\exp\left[j2\pi(q+r)\frac{n_{p',s}-n_{p',s'}}{N}\right]\right|^2$$
$$+\frac{1}{N^2N_s^2}\sum_{s',s=0}^{N_s-1}\left|\sum_{q=-\infty}^{+\infty}\sum_{r=-\infty}^{+\infty} w_0(0;q;r)R(q;r)\exp\left[j2\pi q\frac{n_{p',s}-n_{p',s'}}{N}\right]\right|^2+\frac{N_s-1}{N^2N_s}\left|\sum_{q=-\infty}^{+\infty}\sum_{r=-\infty}^{+\infty} w_0(0;q;r)R(q;r)\right|^2 \tag{28}$$

$$P_T = \frac{K_u}{NN_s}\sum_{q=-\infty}^{+\infty}\sum_{r=-\infty}^{+\infty} w_0(0;q;r)R(q;r)-\frac{N_s-K_u}{N^2N_s(N_s-1)}\sum_{i=-1}^{1}\left|\sum_{q=-\infty}^{+\infty}\sum_{r=-\infty}^{+\infty} w_i(0;q;r)R(q;r)\right|^2$$
$$+\frac{K_u}{N^2N_s^2}\sum_{p=0}^{P-1}\sum_{s',s=0}^{N_s-1}\sum_{i=-1}^{1}\left|\sum_{q=-\infty}^{+\infty}\sum_{r=-\infty}^{+\infty} w_i(n_{p,s}-n_{p',s';}q;r)R(q;r)\exp\left[j2\pi(q+r)\frac{n_{p,s}-n_{p',s'}}{N}\right]\right|^2$$
$$+\frac{N_s-K_u}{N^2N_s^2(N_s-1)}\sum_{s',s=0}^{N_s-1}\left\{\sum_{q=-\infty}^{+\infty}\sum_{r=-\infty}^{+\infty} w_0(0;q;r)R^*(q;r)\exp\left[-j2\pi q\frac{n_{p',s}-n_{p',s'}}{N}\right]\right\}$$
$$\times\left\{\sum_{q=-\infty}^{+\infty}\sum_{r=-\infty}^{+\infty} w_0(0;q;r)\left(\sum_{i=-\infty}^{+\infty}R\left(q-i(N+\nu);r\right)\right)\exp\left[j2\pi q\frac{n_{p',s}-n_{p',s'}}{N}\right]\right\}$$
$$+\frac{N_s-K_u}{N^2(N_s-1)}\sum_{i=-1}^{1}\left|\frac{1}{N_s}\sum_{s'=0}^{N_s-1}\exp\left[j2\pi i n_{p',s'}\frac{\nu}{N}\right]\right|^2\left|\sum_{q=-\infty}^{+\infty}\sum_{r=-\infty}^{+\infty} w_0(0;q;r)R(q;r)\right|^2$$
$$-\frac{N_s-K_u}{N^2N_s(N_s-1)}\left\{\sum_{q=-\infty}^{+\infty}\sum_{r=-\infty}^{+\infty} w_0(0;q;r)\left(\sum_{i=-\infty}^{+\infty}R\left(q-i(N+\nu);r\right)\right)\right\}\left\{\sum_{q=-\infty}^{+\infty}\sum_{r=-\infty}^{+\infty} w_0(0;q;r)R(q;r)\right\} \tag{29}$$

respectively, which are shown at the top of the page. Moreover, the AWGN noise power is

$$P_{\text{AWGN}} = E\left\{\left|\sqrt{\frac{1}{N}}\sum_{s'=0}^{N_s-1}c^*_{p',s'}\gamma^*(n_{p',s'};n_{p',s';}0)\right.\right.$$
$$\left.\left.\times\sum_{k=0}^{N-1}n(k)\exp\left[-j2\pi n_{p',s'}\frac{k}{N}\right]\right|^2\right\}$$
$$= N_0\frac{1}{N}\sum_{q=-\infty}^{+\infty}\sum_{r=-\infty}^{+\infty} w_0(0;q;r)R(q;r). \tag{30}$$

Note that in the expression of the total power in (29), the terms with $w_1(\Delta,q,r)$ [or $w_{-1}(\Delta,q,r)$] are related to anticausal (or causal) part of the channel, i.e., $q<0$ (or $q>0$). This means that for anticausal (or causal) channels, the terms with $w_1(\Delta,q,r)$ [or $w_{-1}(\Delta,q,r)$] will disappear in the expression of P_T in (29). These two contributions belong to the interference power and are not present in the expression of the useful power in (28). Note also that these expressions are valid for any type of mapping between chips and carriers, i.e., $n_{p,s}$. It can be shown that for the mapping that maximizes the distance between the chips corresponding to the same data symbol, i.e., $n_{p,s}=p+sP$, the useful and total powers are independent from the useful symbol p'.

REFERENCES

[1] H. Steendam and M. Moeneclaey, "Analysis and optimization of the performance of the OFDM on frequency-selective time-selective fading channels," *IEEE Trans. Commun.*, vol. 47, no. 12, pp. 1811–1819, Dec. 1999.

[2] H. Sari, G. Karam, and I. J. Claude, "Transmission techniques for digital terrestrial TV broadcasting," *IEEE Commun. Mag.*, vol. 33, no. 2, pp. 100–109, Feb. 1995.

[3] M. Russel and G. L. Stüber, "Terrestrial digital video broadcasting for mobile reception using OFDM," *Wirel. Pers. Commun.*, vol. 2, no. 1/2, pp. 45–66, Mar. 1995.

[4] J. S. Chow, J. C. Tu, and J. M. Cioffi, "A discrete multitone transceiver system for HDSL applications," *IEEE J. Sel. Areas Commun.*, vol. 9, no. 6, pp. 895–908, Aug. 1991.

[5] S. Hara and R. Prasad, "Overview of multicarrier CDMA," *IEEE Commun. Mag.*, vol. 35, no. 12, pp. 126–133, Dec. 1997.

[6] F. Tufvesson and T. Maseng, "Optimization of sub-channel bandwidth for mobile OFDM systems," in *Proc. Multiaccess, Mobility and Teletraffic—Advances Wireless Networks (MMT)*, 1998, pp. 103–114.

[7] Y. H. Kim, I. Song, H. G. Kim, T. Chang, and H. M. Kim, "Performance analysis of coded OFDM system in time-varying multipath Rayleigh fading channels," *IEEE Trans. Veh. Technol.*, vol. 48, no. 5, pp. 1610–1615, Sep. 1999.

[8] G. D. Pantos, A. G. Kanatas, and P. Constantinou, "Performance evaluation of OFDM transmission over a challenging urban propagation environment," *IEEE Trans. Broadcast.*, vol. 49, no. 1, pp. 87–96, Mar. 2003.
[9] H. Steendam, "The effect of synchronization errors on multicarrier systems," Ph.D. dissertation, Ghent Univ., Gent, Belgium, 2000.
[10] R. Steele, *Mobile Radio Communications*. London, U.K.: Pentech, 1992.
[11] K. S. Riedel, "Optimal data-based kernel estimation of evolutionary spectra," *IEEE Trans. Signal Process.*, vol. 41, no. 7, pp. 2439–2441, Jul. 1993.

Mamoun Guenach (S'00–M'02) received the B.S. degree in electronics and communications engineering from the Ecole Mohamadia d'Ingenieurs, Rabat, Morocco, in 1995 and the M.S. degree in electricity and the Ph.D. degree from the Universite Catholique de Louvain, Louvain, Belgium, in 1998 and 2002, respectively.

He was a Consultant Engineer at the Chamber of Commerce and Industry of Morocco from 1996 to 1997. He is currently a Postdoctoral Researcher in the Department of Telecommunications and Information Processing, Ghent University, Gent, Belgium. His main research interest is iterative detection/synchronization/estimation for coded systems.

Heidi Steendam (M'01) received the M.Sc. degree in electrical engineering and the Ph.D. degree in applied sciences from Ghent University, Gent, Belgium, in 1995 and 2000, respectively.

Since October 2002, she has been a full-time Professor in the Digital Communications (DIGCOM) Research Group, Department of Telecommunications and Information Processing (TELIN), Ghent University. She is the author of more than 70 scientific papers published in international journals and conference proceedings. Her main research interests are in statistical communication theory, carrier and symbol synchronization, bandwidth-efficient modulation and coding, spread spectrum (multicarrier spread spectrum), and satellite and mobile communications.